Simulation aided development of pre-chamber ignition system for a lean-burn gasoline direct injection motor-sport engine

Muhammed Fayaz Palakunnummal
PhD Research Student
School of Engineering
London South Bank University
UK
Email: palakunm@lsbu.ac.uk

Priyadarshi Sahu
PhD Research Student
School of Engineering
London South Bank University

Mark Ellis
Senior Lecturer
School of Engineering
London South Bank University

Marouan Nazha
Emeritus Professor
School of Engineering
London South Bank University

Due to recent regulation changes to restricted fuel usage in various motor-sport events, motor-sport engine manufacturers have started to focus on improving the thermal efficiency and often claim thermal efficiency figures well above equivalent road car engines. With limited fuel allowance, motor-sport engines are operated with a lean air-fuel mixture to benefit from higher cycle efficiency, requiring an ignition system that is suitable for the lean mixture. Pre-chamber ignition is identified as a promising method to improve lean limit and has the potential to reduce end gas auto-ignition. This paper analyses the full-load performance of a motor-sport lean-burn GDI engine and a passive pre-chamber is developed with the aid of a CFD tool. ***The finalized pre-chamber design benefited in a significant reduction in burn duration, reduced cyclic variation, knock limit extension and higher performance.***

Nomenclature

ATDC After top dead center.
BSFC Brake specific fuel consumption.
CFD Computational fluid dynamics.
GDI Gasoline direct injection.
HCCI homogenous charge compression ignition.
IMEP Indicated mean effective pressure.
KLSA Knock limited spark advance.
MBF Mass burnt fraction.
MBT Minimum advance for best torque.
PFI Port fuel injection.
LES Large eddy simulation.
RANS Reynolds averaged Navier Stokes.
TDC Top dead center.
λ Relative equivalence ratio

1 Introduction

Motor-sport engines can show a direction for how gasoline engines can be designed for achieving higher thermal efficiency. To make motor-sports road relevant and to attract automotive manufactures, motor-sports regulatory authorities including International Auto-mobile Federation (FIA) recently started focusing on fuel efficiency. This was

done by restricting the maximum fuel flow rate to the engine and also by limiting total fuel quantity for a race or per stint for longer running endurance races [1]. Such a restriction has resulted in motor-sport engine manufacturers focusing on reducing the brake specific fuel consumption (BSFC). As per Formula One engine regulations, cylinder geometry including the compression ratio is defined and restricted [1]. So one possible direction to reduce the BSFC is to increase the dilution. The 1.6 Liter V6 Formula One engine introduced in 2014 is permitted to use a maximum fuel flow rate of 100 kg-hr. Formula One engine manufactures often claim thermal efficiency figures well above an equivalent road car engine. Though major efforts went into developing these highly efficient engines, research findings are not available in the public domain or published literature. Motor-sport engines operate mostly at full load and in a narrow engine speed range, where it is convenient to design an engine for higher efficiency compared to a wider load and speed range automotive engine. Such an engine with a narrow operating range can also find its use in hybrid vehicles where electric assist allows the engine to operate only on efficient operating points. Various studies predicted that by 2050, around 60 to 70% of passenger cars still be powered by hybrid power-trains, with a major contribution from gasoline-hybrid power-trains [2], [3].

Though not available in any published form, it is plausible Formula One engines use high energy ignition systems like pre-chamber ignition system. A study of pre-chamber ignition system on a motor-sport engine can hence identify the potential of future power-trains in achieving higher thermal efficiency. The discussion of this paper is organized as follows: first, a review of previous works done on the pre-chamber ignition system. Second, a discussion on full load performance of a spark ignited turbocharged lean-burn Gasoline Direct Injection (GDI) motor-sport engine and analyzing how a pre-chamber can better combustion compared to normal spark ignition. Third, A computational fluid dynamics (CFD) based parametric study to develop a passive pre-chamber design and fourth, validation of pre-chamber model with the test results.

2 Pre-chamber ignition systems

A pre-chamber is an auxiliary small volume combustion chamber with multiple orifices connecting to the main combustion chamber, with a spark plug mounted inside, with or without an injector inside and usually replaces the normal spark plug in a gasoline engine. In pre-chamber ignition system, multiple turbulent flame jets from a pre-chamber burn main combustion chamber mixture in much shorter duration compared to a conventional spark ignition system [4]. The shorter burn duration reduces end gas residence time at elevated pressure and temperature and hence has the potential to reduce the engine knock. The pre-chamber jet ignition concept involves the use of a chemically active, turbulent jet to initiate the combustion in lean fuel mixtures. The hot reacting jet produced by turbulent jet ignition has two effects on combustion in the main chamber. First, the generation of turbulence produced by the shear of the jet flow increases the flame propagation speed. Second, the jet distributes hot gases over a wide region in the main chamber which generates distributed ignition throughout the chamber where the jet has passed [4]. The higher number of distributed ignition sites ensure that the flame travel distances are relatively small enabling short combustion duration, even in slow-burning lean mixtures.

Thelen et al. [5] studied the influence of orifice size in a pre-chamber and observed that smaller orifices produce faster burn rates, mainly attributed to the increased amount of turbulence generated by higher velocity jets. Thelen et al. [6] also investigated the optimum spark plug location inside the pre-chamber and concluded that ignition source must be located as far away from the orifice as possible while maintaining good scavenging near the spark plug.

If the main objective is to achieve lean burn combustion, it is necessary to have good combustible mixture near the spark plug. This requirement is also valid for a pre-chamber ignition system where pre-chamber ignition is initiated by a spark plug. In a study by Gussak [7], it was identified that the availability of active radicals in the pre-chamber jets increased as the mixture in the pre-chamber was made richer, up to a certain limit. This work also identified that jets of hotter, but complete combustion products are generated when a stoichiometric or slightly leaner mixture is burned inside the pre-chamber. These jets had significantly lower combustion performance compared to burning rich mixture inside the pre-chamber. So higher overall lean mixture necessitates an arrangement to achieve rich mixture inside the pre-chamber. This can be done either by making a stratified mixture by spray or wall guided injection. Kettner et al. [8] used a Bowl Pre-chamber Ignition concept with a bowl on the piston and multi-stage fuel injection to guide fuel towards the pre-chamber.

An alternative method to ensure rich mixture inside the pre-chamber is to have separate fuel injection inside the pre-chamber. Injecting liquid fuel inside the pre-chamber is a challenging task due to less space available for vaporization and homogeneous mixture formation. William Attard did extensive studies on turbulent jet ignition with pre-chamber injection [9] [10] [11] [12] [13]. Such an arrangement is not considered here as it would require a separate fuel delivery system to achieve the optimized spray parameters inside a small volume pre-chamber. An additional fuel delivery system is not a preferred option for a motor-sport engine due to weight increase and complexity. Use of more than one injector per cylinder is also restricted for most of the motor-sport engines including Formula one engine [1].

Attard et al. [11] compared knock limit of conventional spark ignition and pre-chamber jet ignition by reducing fuel quality on a Port Fuel Injection (PFI) engine. Different

Primary Reference Fuel with varying octane number was tested on a stoichiometric normally aspirated engine at full load. With a passive pre-chamber system, 10 octane number improvement was reported at Minimum advance for Best Torque (MBT) ignition timing. The reported reduction in MBF10-90% duration was around 50%.

Attard et al. [12] observed that pre-chamber distributed ignition can result in higher pressure rise rates, beyond the acceptable limit of spark-ignition engines, placing increased loading on components. This is somewhat identical to the difficulty in operating at full load with a Homogeneous Charge Compression Ignition (HCCI) engine. Nevertheless, this pressure rise rate can be controlled in different ways, for example, delaying ignition timing. This limitation implies achieving the shortest burn duration must not be the sole criteria and pressure rise rate must be controlled to a tolerable limit.

A pre-chamber ignition system has a potential drawback in scavenging pre-chamber, especially at part load operating points [14]. Geiger et al. [15] observed that at part load operating points, the pre-chamber function is adversely affected because of high residual fraction inside the pre-chamber due to poor scavenging.

Although jet ignition systems provide additional ignition energy, additional surface area of the pre-chamber increases the heat transfer loss and can hence reduce the Indicated Mean Effective Pressure (IMEP), if the same combustion phasing is used [10]. This increased heat transfer can reduce thermal efficiency if no design changes are made to benefit from the increased knock resistance or increase the dilution.

To summarize this section, the main contribution of a pre-chamber is identified as the reduced burn duration. The benefit of reduced burn duration could be significant with a lean burn engine as lean mixture has increased burn duration compared to an engine operating near the stoichiometric level. Pre-chamber ignition systems reduce burn duration by around 50% over the base spark ignition arrangement. But this reduced burn duration does not necessarily convert in to gain in IMEP, as its benefit is outdone by increased heat transfer loss. Another reported benefit is knock limit extension with the reduced residence time of end gas. A higher compression ratio or increased dilution can benefit from reduced knock occurrence and stable combustion possible with the pre-chamber ignition systems, hence possible to increase the IMEP over the base engine. Pre-chamber performance is largely influenced by the mixture state inside the pre-chamber and rich mixture (relative equivalence ratio, $\lambda<1$) is essential inside the pre-chamber for good combustion performance.

3 Full load performance of a motor-sport engine

In this section, the full-load performance of a motor-sport engine is reviewed and scope of performance improvement is analyzed. For a fuel flow restricted motor-sport engine, the primary objective of the design is to reduce the BSFC to the lowest level possible. To achieve a lower BSFC, compression ratio and relative equivalence ratio (λ) is increased until its benefit is outdone by spark knock and cyclic variation respectively.

A single-cylinder research engine was developed based on an existing V6 turbocharged spark-ignition GDI motor-sport engine at London South Bank University. The single-cylinder research engine design specifications were modified from its base engine to give a consistent performance. This single cylinder engine has a geometrical compression ratio of 13 and can operate at relative equivalence ratio (λ) up to 1.4. Key engine geometry specifications are provided in Table 1. Additional engine design specifications are not discussed here due to engine design confidentiality. Also, normalized cylinder pressure curves are used in this paper for the same reason. A two-stage supercharger rig powered by the engine dyno and an exhaust back pressure valve is used to simulate the turbo-charged air supply of the base engine. AVL X-ion data acquisition system and AVL CONCERTO is used to measure and post process cylinder pressure data. The engine calibration was done ensuring constant fuel flow rate at all the speed points tested. A schematic diagram of engine test set-up, explaining signals to achieve target fuel flow rate is given in Fig. 1. The base engine calibration parameters including fuel injection timing, injection pressure, relative equivalence ratio were finalized to achieve the lowest BSFC at target fuel flow rate. The ignition timing is decided by knock limited spark advance (KLSA) and knock is detected by a surface mounted transducer based knock sensor. The measured cylinder pressure data of 100 cycles for the average engine speed (7000 rpm, full-load and $\lambda = 1.2$) is shown in Fig. 2. Another plot of maximum, minimum and average pressure profile for the same measurement is shown in Fig. 3.

Combustion chamber	Pent-roof with bowl piston
Compression ratio	13.0
Maximum operating speed	8000
Displacement	500 cc
Fuel	Gasoline with 20% ethanol
Number of valves per cylinder	4
Max. fuel injection pressure	500 Bar

Table 1. Design specifications of the single cylinder research engine

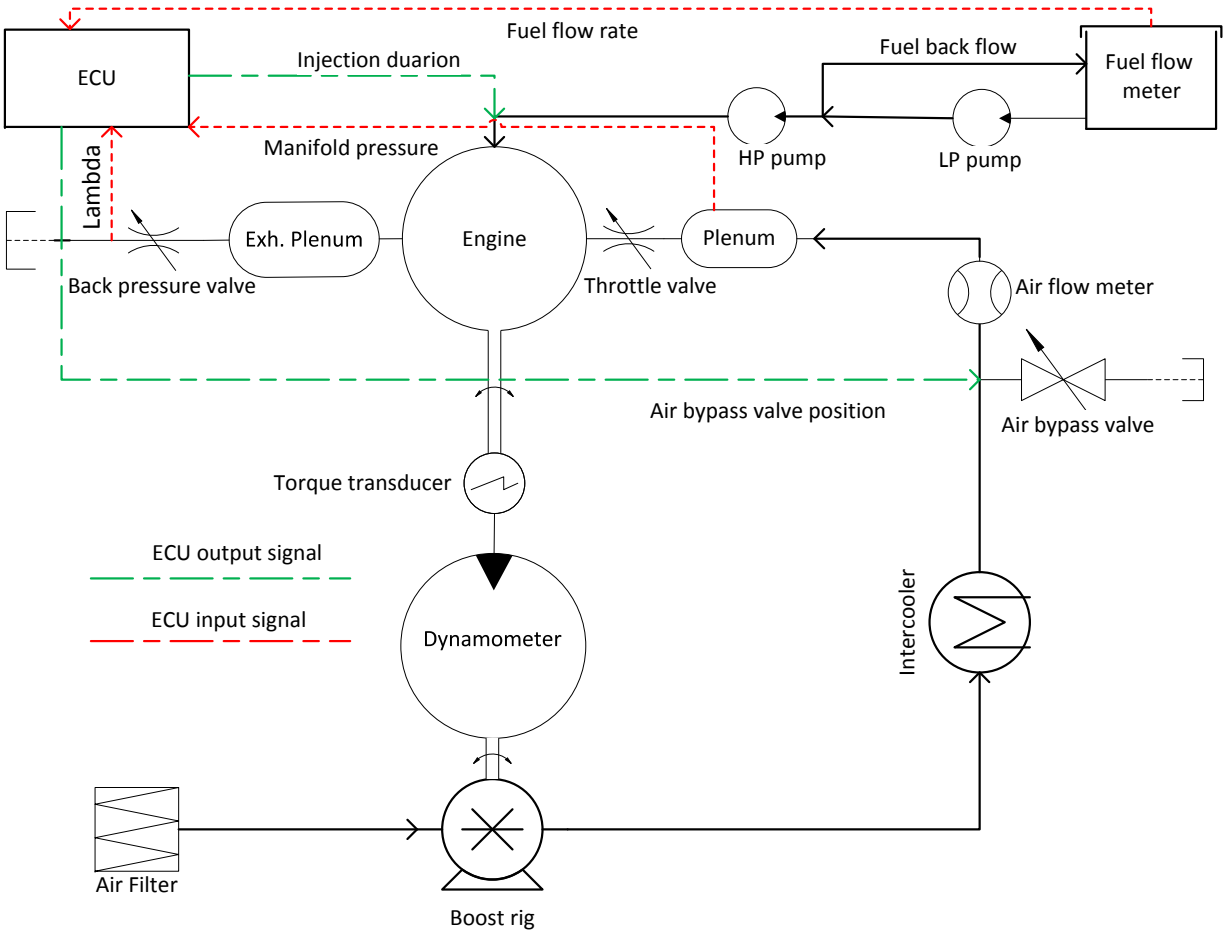

Fig. 1. Schematic diagram of single cylinder engine test set-up. Various signals and actuators to maintain fuel flow rate at full-load are shown.

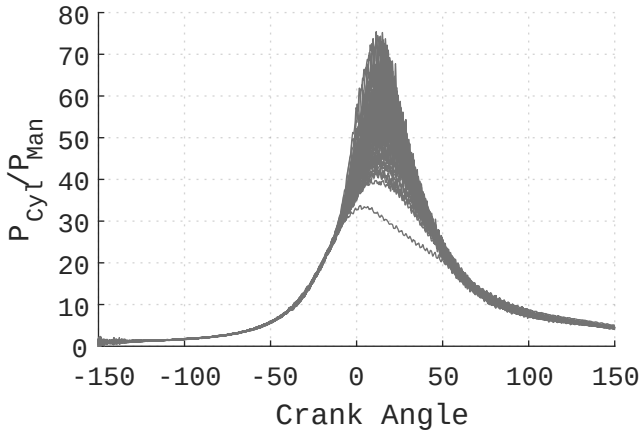

Fig. 2. Measured cylinder pressure data (unfiltered) for 100 cycles, normalized with intake manifold average pressure.

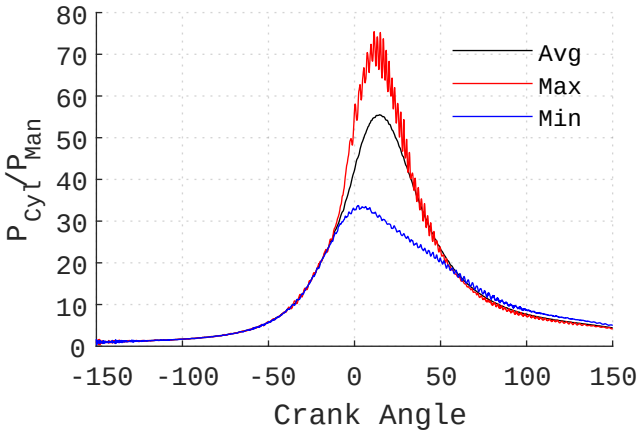

Fig. 3. Minimum, maximum and average pressure curves from 100 test cycles. Maximum pressure curve (red) is a knocking cycle with knock initiated at 15^{o} ATDC.

The pressure curve with highest peak pressure in Fig. 3 represents a knocking cycle and is detected by transducer based knock sensor which limits the ignition timing advance. The pressure curve with the lowest peak pressure represents a misfire cycle or much delayed combustion which decides the lean limit an engine can operate. The declared performance and BSFC figures are decided by

the average pressure curve. Thus, a reduction in cyclic variation can increase the average pressure profile for a given knock limit. Alternatively, extending the lean limit for the allowed cyclic variation (eg: CoV of IMEP) can also raise the average pressure profile and achieve a lower BSFC. Average pressure curve can also be raised by improving knock resistance of the engine.

The total elimination of cyclic variation is not necessary, as it is acceptable to the engine only a few cycles to knock [16]. Full load calibration of a motor-sport engine is done by allowing a few cycles to knock with the threshold is decided based on the rebuild interval of the engine. In a literature study by Ozdor et al. [17] and in a LES based numerical study by Truffin et al. [18], it was identified that changes in the flow convection near the spark plug as the most influential factor causing cyclic variation of combustion start. It is widely accepted that the early flame development can have a profound effect on the combustion duration [16]. With a pre-chamber ignition system, flow field inside the pre-chamber is decided by the reverse jet flow from the main chamber to the pre-chamber during the compression stroke and variation in large flow structures outside the pre-chamber is not communicated inside the pre-chamber. Compression pressure curves are repetitive as shown in Fig. 2, ensuring constant pressure difference across the chambers for all cycles. Thus, a pre-chamber ignition system has the potential to reduce or eliminate cycle to cycle flow variations near the spark plug, which is located inside the pre-chamber.

Lean mixture ($\lambda > 1$) reduces flame velocity and increases the burn duration. The reduced burn duration widely reported with the pre-chamber ignition is a promising solution for lean operation, and it can help in placing peak pressure points closer to TDC. Furthermore, a fast burning combustion process significantly reduces the impact of combustion cyclic variation on engine performance [19].

Chinnathambi et al. [20] observed that jet penetration length is reduced with the increased cylinder pressure. This could be an adverse factor for implementing the pre-chamber on motor-sport engines as these engines are usually run with high manifold pressure and resultant higher cylinder pressure before combustion start, and can result in reduced jet penetration.

Philip et al. [21] observed that interaction of fluctuating flow and direct-injected spray leads to a substantial increase in cyclic differences of the in-cylinder flow, which affects spray penetration and mixture formation. Goryntsev et al. [22] also studied the interaction of injected fuel spray jet and cylinder charge motion and observed considerable changes in the intensity of cyclic fluctuation at the center of tumble motion. The same study also reported significant cyclic variations in the air-fuel mixing process, fuel jet penetration and forming of fuel vapor cloud near the spark plug. So any changes in the flow field and mixing can result in spark plug seeing different mixture state from cycle to cycle. This variation in mixture state near the spark plug is not eliminated even with a pre-chamber, as the mixture state inside the pre-chamber depends on the instantaneous mixture state in the vicinity of the pre-chamber during the compression stroke and filling of the pre-chamber occurs through the reverse jet flow from the main combustion chamber to the pre-chamber. For a pre-chamber based engine operating at lean mode, effect of different mixture state inside the pre-chamber from cycle to cycle could be substantial, as different mixture state can result in different burn duration of pre-chamber charge and resultant jet ejection time from the pre-chamber, which is the start of combustion in the main chamber. The possible remedy is to ensure a rich mixture ($\lambda < 1$) near the pre-chamber nozzles during the compression stroke, either using spray guided, wall guided or using a split injection, which would ensure rich mixture near the pre-chamber nozzles.

4 Single cylinder CFD model

CFD tools with the capabilities to model spray and combustion are very useful in studying the pre-chamber performance. This numerical methodology is more relevant for pre-chamber combustion, because such a small volume has difficulty in instrumentation, as observed by Chinnathambi et al. [20] that a small tunnel used for the pre-chamber pressure measurement acted as knock initiation site inside the pre-chamber. An in-cylinder CFD model for the single cylinder research engine is developed in CONVERGE CFD code and further modified to evaluate different pre-chamber designs. A parametric study was conducted with the CFD model to optimize the different design features of a passive pre-chamber design. CONVERGE is a general purpose CFD code for the calculation of three-dimensional, compressible, chemically reacting fluid flows in complex geometries with stationary or moving boundaries. This solver can handle an arbitrary number of species and chemical reactions, as well as transient liquid sprays and turbulent flows. A modified cut-cell Cartesian method is used that eliminates the need for the body fitted computational cells with the geometry of interest. This method allows for the use of simple orthogonal grids and completely automates the mesh generation process [23]. This finite volume based code provides various model options for turbulence, spray formation and combustion chemistry [23]. The RNG $k-\varepsilon$ model was used to capture sub grid scale influence of turbulence on the momentum, energy and species transport fields.

Pressure velocity coupling is achieved through Pressure Implicit with Splitting of Operators (PISO) method. The two-phase spray process is calculated using an Eulerian-Lagrangian approach, included in the CFD code [23]. Basic spray modeling options with minimum tuning coefficients available with the code were used and no separate validation of spray formation was done due to the unavailability of a dedicated spray experiment set up. The E20 gasoline fuel

used for the experiment is represented by iso-octane (80%) and ethanol (20%) in simulation.

The SAGE detailed chemistry solver [24], available with the CONVERGE CFD code was used to perform the combustion calculation. The SAGE solver models detailed chemical kinetics via a set of CHEMKIN [25] formatted chemical reaction mechanism files. The skeletal mechanism used for this study is built by merging a mechanism of toluene reference fuel [26] and an ethanol mechanism [27] and has used 63 species and 207 reactions for combustion calculation. Budak et al. [28], in their study, have validated the SAGE solver coupled with CONVERGE CFD for predicting combustion in a boosted GDI engine. Spark ignition is modeled by introducing an energy source at the spark plug tip in a defined volume and duration and this energy source is allowed to move near the spark plug, simulating flame kernel shifting with the flow.

The base cell size of 2 mm was used for the engine cylinder geometry shown in Fig. 4. Local grid refinements

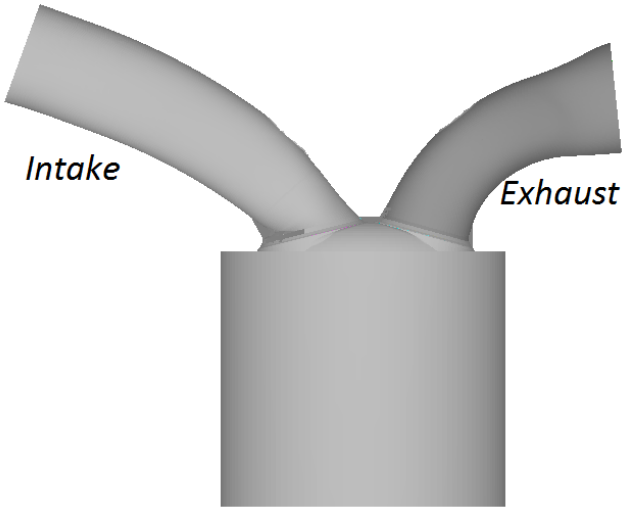

Fig. 4. CFD geometry for the combustion chamber and ports

were utilized near the regions where sharp gradients in flow variables were expected such as spark plug, valve seats etc. The smallest cell size used in this study is 0.125 mm, which is near the spark plug during the combustion start and also inside the pre-chamber and in the area where pre-chamber jets eject in to the main combustion chamber. For a typical engine simulation with a RANS based turbulence model, it was identified that increasing mesh resolution beyond 0.1 mm would not improve the accuracy as there are no more scales to resolve [29]. Inlet and outlet port pressure and temperature boundary conditions were used from a correlated GT Power model of the same engine. For a pre-chamber simulation, the maximum number of cells has reached 3.5 million. The simulations were run in a 48 core cluster computer and the run time was 80 hours for one four-stroke cycle with pre-chamber combustion.

4.1 Correlation to measurement

A well correlated CFD model is expected to show the exact behavior of pressure curves as observed in the test data (Fig. 2). Previous studies identified that LES based simulations can quantitatively predict cyclic variation [30], [18]. A Reynolds Averaged Navier Stokes (RANS) based CFD model tends to be more diffusive and does not achieve a quantitative correlation to cyclic variation and stays close to the average pressure curve. However, previous studies have shown that cyclic variations is visible in engine combustion with RANS turbulence model if the scales of the flow that are causing the cyclic variations are not small enough to be destroyed by the RANS turbulence viscosity [31], [32]. Scarcelli et al. concluded that with a well refined mesh, low numerical viscosity can be achieved and RANS based engine model can show cyclic variability which comes from the variability of large flow structures from cycle to cycle [33]. As discussed in the previous section, changes in mean flow field and its interaction with spray are the most influential factors causing cyclic variations in a GDI engine. The base motor-sport engine was developed with high intake valve seat masking to induce tumble and as this engine operates at higher speeds, the result is very high mean tumble velocity inside the cylinder during the intake and compression strokes. Thus, any changes inside the cylinder during intake valve opening contributed from the previous cycle combustion event can be amplified which results in different flow field from cycle to cycle. So despite using a RANS model, it is not necessary to get an ensemble averaged result after a few cycles. Multi-cycle simulated cylinder pressure data for the base spark ignition engine is compared with the measurement data as shown in Fig. 5. **Average pressure**

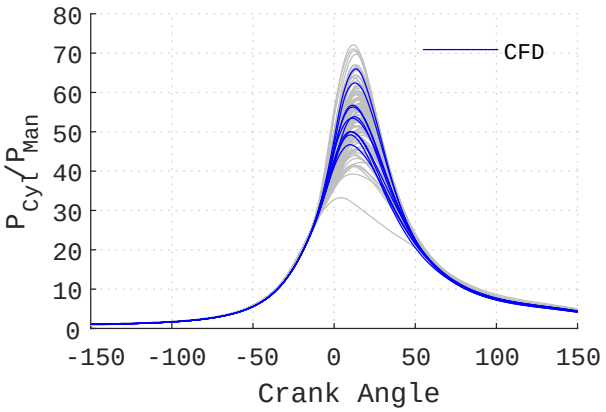

Fig. 5. 10 continues simulated cycles compared with 100 cycles of measured data. Measured pressure (filtered) data is shown in light gray color.

curve for the same 10 simulated cycles achieved close

correlation with the measured average data as shown in Fig. 6. First cycle simulated data is not considered to avoid the influence of initialization variables used. It can be seen that pressure curves up to the combustion start is repetitive, but they start to deviate from the average pressure curve from the combustion start, with reduced peak pressure variation compared to the measurement data. **Inlet tumble flow observed to be fluctuating from cycle to cycle and its interaction with spray, resulting in different mixture distribution at combustion start. Both flow and mixing variations influencing local conditions near the spark plug and resulting in variations in ignition delay and burn duration, cycle to cycle.**

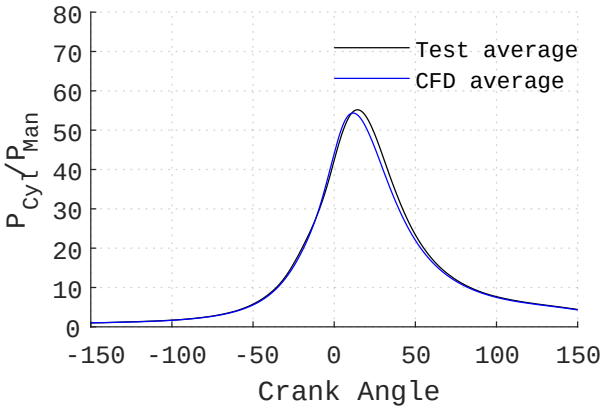

Fig. 6. Average of 10 simulated cycles and 100 test cycles.

5 Pre-chamber design optimization

The base engine CFD model was modified to include a pre-chamber design and a parametric study was conducted to decide the design features of the pre-chamber including position of the pre-chamber within the combustion chamber, pre-chamber volume, number of nozzles, nozzle diameter and nozzle orientation. Simulations were conducted for designs with different combinations of all above variables. For each design, simulation were performed for three consecutive cycles. First cycle result was omitted to eliminate the influence of initialization variables used in the CFD case set up and the average of the last two cycles was considered for the discussion to account for cycle to cycle variation as discussed in the previous section. Most of the pre-chamber designs evaluated show a substantial reduction in burn duration ($MBF10-90\%$) over the base spark plug ignition system. This much reduced burn duration results in heavy knocking if the ignition angle of the base spark plug model is used. Hence, all the pre-chamber simulations are done with a 10 deg ignition retard from the base ignition angle. The cases that achieved a burn duration angle less than 25^o are the result of knocking combustion from a shorter ignition delay and a much reduced burn duration and which requires further spark retard for actual implementation. Fig. 7 explains the order of each design variable finalized with objective from each design feature mentioned. Following sections discuss the influence of each design variable in detail.

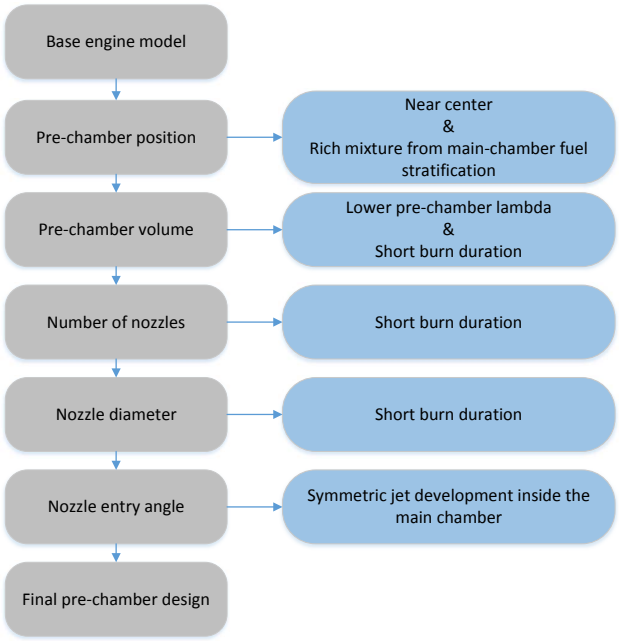

Fig. 7. Pre-chamber design iteration steps with objectives from each design features mentioned on the right.

5.1 Pre-chamber position

The base motor-sport sport engine operates at higher engine speeds ($> 6000\,RPM$) and thus time available for fuel injection and mixture formation is less. Higher injection pressure (up to 500 bar) is utilized to complete fuel injection in less time available and also to improve mixing but still results in a stratified mixture state as shown in Fig. 8. For the base engine, the spark plug is positioned on the intake side to benefit from the presence of rich mixture on the intake side. Placing the spark plug on the intake side can increase the knock occurrence as the exhaust side of the combustion chamber tends to be at a higher temperature state compared to the intake side. But with spark plug ignition system, the presence of active tumble flow field during the combustion start (Fig. 9) helps in convecting flame towards the exhaust side which allows the air-fuel charge on the exhaust side burns first, as shown in Fig. 10. To benefit from the rich mixture on the intake side, the pre-chamber was placed on the base spark plug location. Since the pre-chamber ignited flame development inside the main chamber is uniform from the pre-chamber, the flame development was found to be shifted towards the intake side because the pre-chamber is located on the intake side (Fig. 11). Pre-chamber ignited flame was less convected by the main combustion chamber

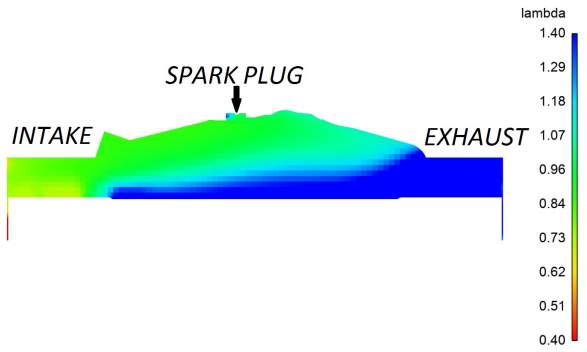

Fig. 8. Relative equivalence ratio on a mid cylinder plane normal to crank axis at combustion start with intake and exhaust sides marked.

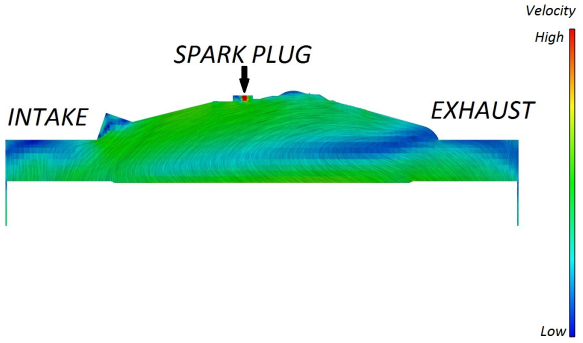

Fig. 9. Line Integral Convolution (LIC) visualization of flow field on a mid cylinder plane normal to crank axis at combustion start.

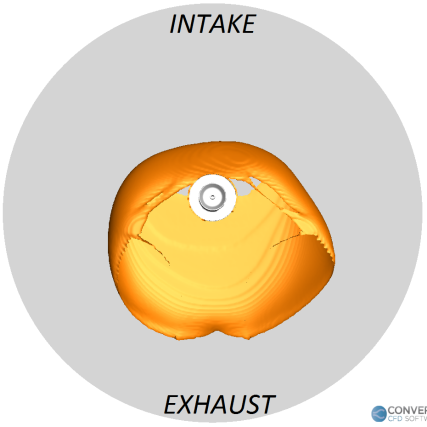

Fig. 10. Spark plug ignited flame development at TDC (CFD result, temperature iso-surface = 1700 K).

flow field. Such a flame development results in the mixture present in the exhaust side to burn towards the end and thus result in increasing knock level, as shown in Fig. 12.

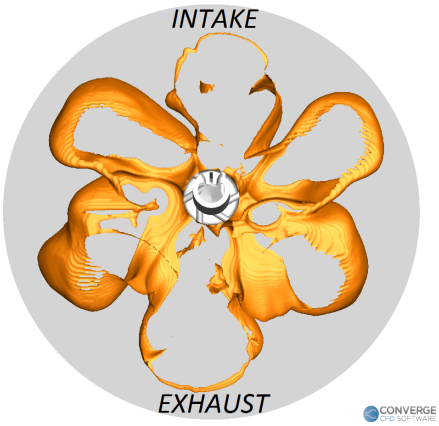

Fig. 11. Pre-chamber ignited flame development at TDC (CFD result,temperature iso-surface = 1700 K).

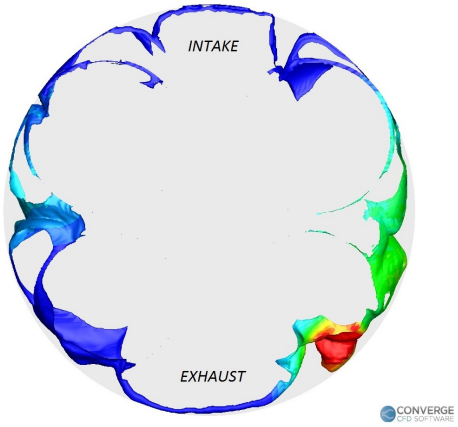

Fig. 12. Flame state at knock onset (CFD result, CA= 16 ATDC, temperature iso-surface of 1700 K, colored by the pressure difference between mean cylinder pressure and local pressure values). Red colored area shows knock initiated flame ahead of pre-chamber initiated flame.

5.2 Pre-chamber volume

Pre-chamber volume from 0.5 cc to 1.5 cc was evaluated and it was observed that with the increasing pre-chamber volume, burn duration is reduced (Fig. 13). The reason is higher charge mass inside the pre-chamber volume results in higher pre-chamber pressure and resultant increased jet penetration inside the main chamber. But as the pre-chamber volume is increased, the mixture state was observed to be leaner and also have higher variations from case to case (Fig. 14) and also cycle to cycle. Lean mixture state inside the pre-chamber is not ideal for the pre-chamber performance as discussed in the section before. Simulation results also show that pre-chamber has around 5% exhaust residuals compared to 2% inside the main chamber, showing difficulty in scavenging and significance of maintaining rich mixture inside the pre-chamber. The predicted combustion start angle for the main combustion chamber is shown in Fig. 15.

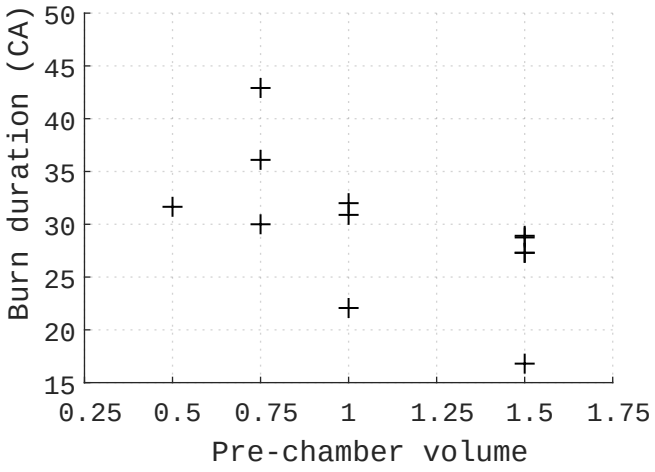

Fig. 13. Burn duration angle (MBF10-90%) vs pre-chamber volume.

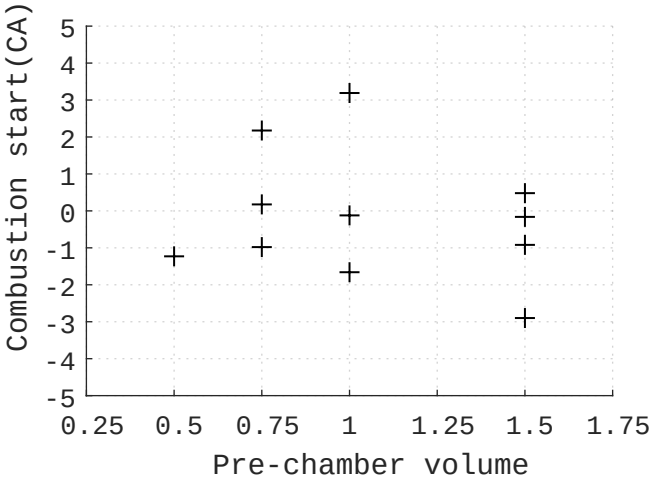

Fig. 15. Combustion start angle (MBF10%) vs pre-chamber volume, Crank angle is with respect to TDC firing.

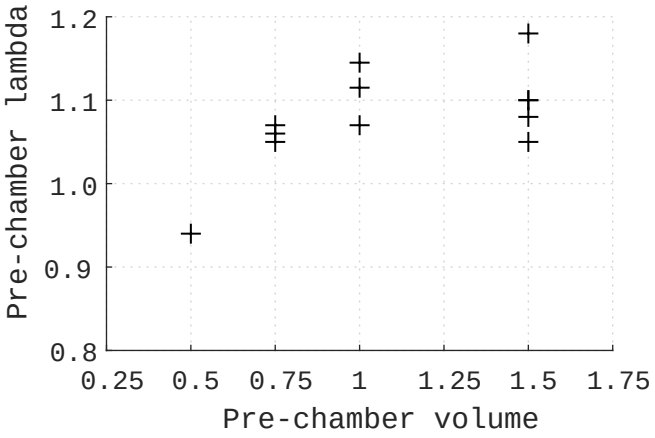

Fig. 14. Relative equivalence ratio (lambda) vs pre-chamber volume.

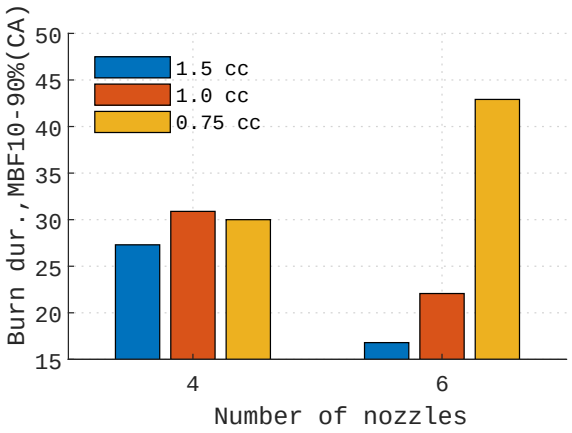

Fig. 16. Burn duration vs number of nozzles and pre-chamber volume

5.3 Number of nozzles

The influence of number of nozzles on burn duration was observed to be a function of pre-chamber volume. A design with less number of nozzles was found to be effective with a smaller pre-chamber volume and vice versa (Fig. 16). A design with higher number of nozzles and a smaller volume doesn't allow pressure to build up inside the pre-chamber. The trend has shown that the number of nozzles can be increased with increasing the pre-chamber volume.

5.4 Nozzle diameter

For the range of the pre-chamber volumes considered, 1.5 mm diameter was observed to be the optimum diameter (Fig. 17). A smaller diameter nozzle with a large volume pre-chamber was found to limit jet penetration despite having higher pressure inside the pre-chamber, as shown in Fig. 18. Fig. 18 also shows reduced pressure inside the pre-chamber with smaller diameter during compression and increased pressure after combustion inside the pre-chamber due to higher restriction of nozzles, both can be attributed to increased pressure drop across the smaller diameter nozzles.

5.5 Nozzle angle

Tangential nozzle entry was observed to improve mixing inside the pre-chamber and helped in symmetrical jet ejection from the pre-chamber as shown in Fig. 19. For asymmetrical jet ejection, the late ejecting jets have reduced penetration length due to decreased pressure inside the pre-chamber from the earlier ejected jets. The end gas in the main chamber in the path of the late ejecting jets would be exposed to higher pressure for a longer duration, thus increasing the probability of auto-ignition.

5.6 Final design

The parametric study revealed that a larger volume pre-chamber has the ability to reduce the burn duration substan-

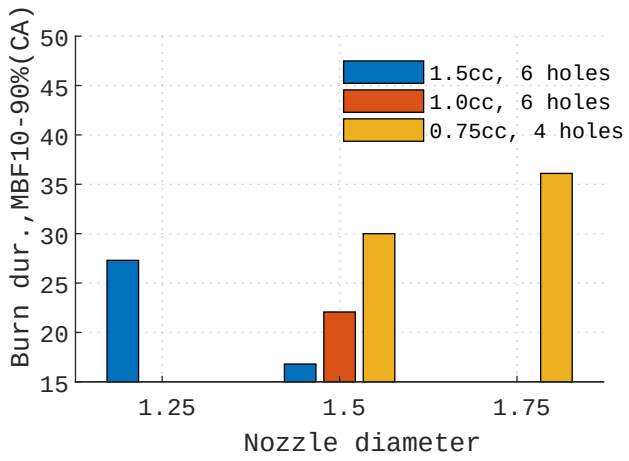

Fig. 17. Burn duration vs nozzle diameter (1.25,1.5 and 1.75 mm) and pre-chamber volume

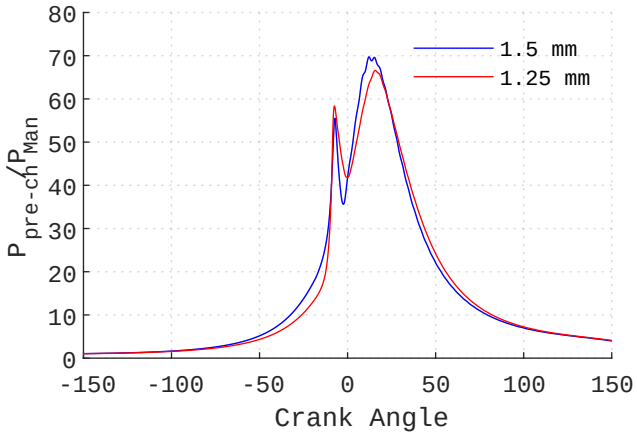

Fig. 18. Pre-chamber pressure for 1.5 mm and 1.25 mm nozzle cases (1.5 cc volume)

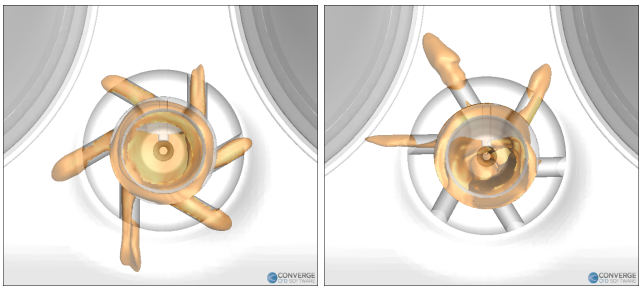

Fig. 19. Influence of nozzle angle on jet flame development Left: Tangential entry nozzles, right: Reduced entry angle or radially aligned nozzles.

tially, but results in a lean mixture inside the pre-chamber which is not ideal for combustion stability. Very short burn duration with varying combustion start is not desirable for an engine which always operates close to knock limit. Based on this observation, the following two pre-chamber designs were tested for validation.

Pre-chamber 1: 1.2 cc pre-chamber volume, 6 nozzles, 1.5 mm nozzle diameter with tangential nozzle entry.

Pre-chamber 2: 0.8 cc pre-chamber volume, 4 nozzles, 1.5 mm nozzle diameter with tangential nozzle entry.

The option 1 was expected to give shorter burn duration with high cyclic variation. With the second option, moderate burn duration and reduced cyclic variation was expected.

6 Test validation of pre-chamber designs

The finalized pre-chamber designs were tested on the base engine at two full-load speed points: 6000 and 7500 rpm. These two test speed points were different from the speed point at which the simulations were conducted. This was due to belt resonance and resultant failure observed with the supercharger rig at 7000 rpm. The two speed points that were tested were on either side of the engine speed at which the simulations were conducted. As both test points were run at the same fuel flow rate of 13.32 kg-hr (single cylinder flow corresponding to 80 kg-hr for the V6 engine), at higher speed, the engine uses less fuel per cycle which resulted in reduced IMEP. Manifold absolute pressure is above 2.0 Bar for both the test points.

Spark ignition tests were run by identifying knock limited spark advance (KLSA). With the pre-chamber ignition, the transducer based knock signals were observed to be very noisy. This was due to additional high frequency oscillations associated with the pre-chamber jets, which appear in the same frequency range of knock excited vibrations. So with the pre-chamber combustion, ignition timing was decided by listening to engine knock noise and also by observing cylinder pressure traces. With the pre-chamber ignition, KLSA was not achieved as it requires momentary ignition retard to prevent runaway knock while running at KLSA, which was not possible as knock sensor signals were noisy. So for actual implementation, an alternate knock detection strategy like cylinder pressure based methods would be required to get the best performance from the engine. With the pre-chamber ignition, knocking was not observed at 7500 rpm and ignition timing was decided by the MBT ignition timing. For pre-chamber testing, all calibration parameters other than ignition timing were kept the same as the base spark plug case.

The measured cylinder pressure for both speed points are shown in Fig. 20. The comparison of average pressure curves are shown in Fig. 21 and Fig. 22. The comparison of CoV of IMEP and maximum pressure is shown in Fig. 23 and Fig. 24. Ignition delay and burn duration comparison is shown in Fig. 25 and Fig. 26. With pre-chamber 2, lower CoV and higher IMEP was achieved at both speed points over the base spark ignition case. Despite having identical ignition delay and reduced burn duration as pre-chamber 2, pre-chamber 1 produced less IMEP than the base spark ignition case. Pre-chamber 1 resulted in higher CoV of IMEP

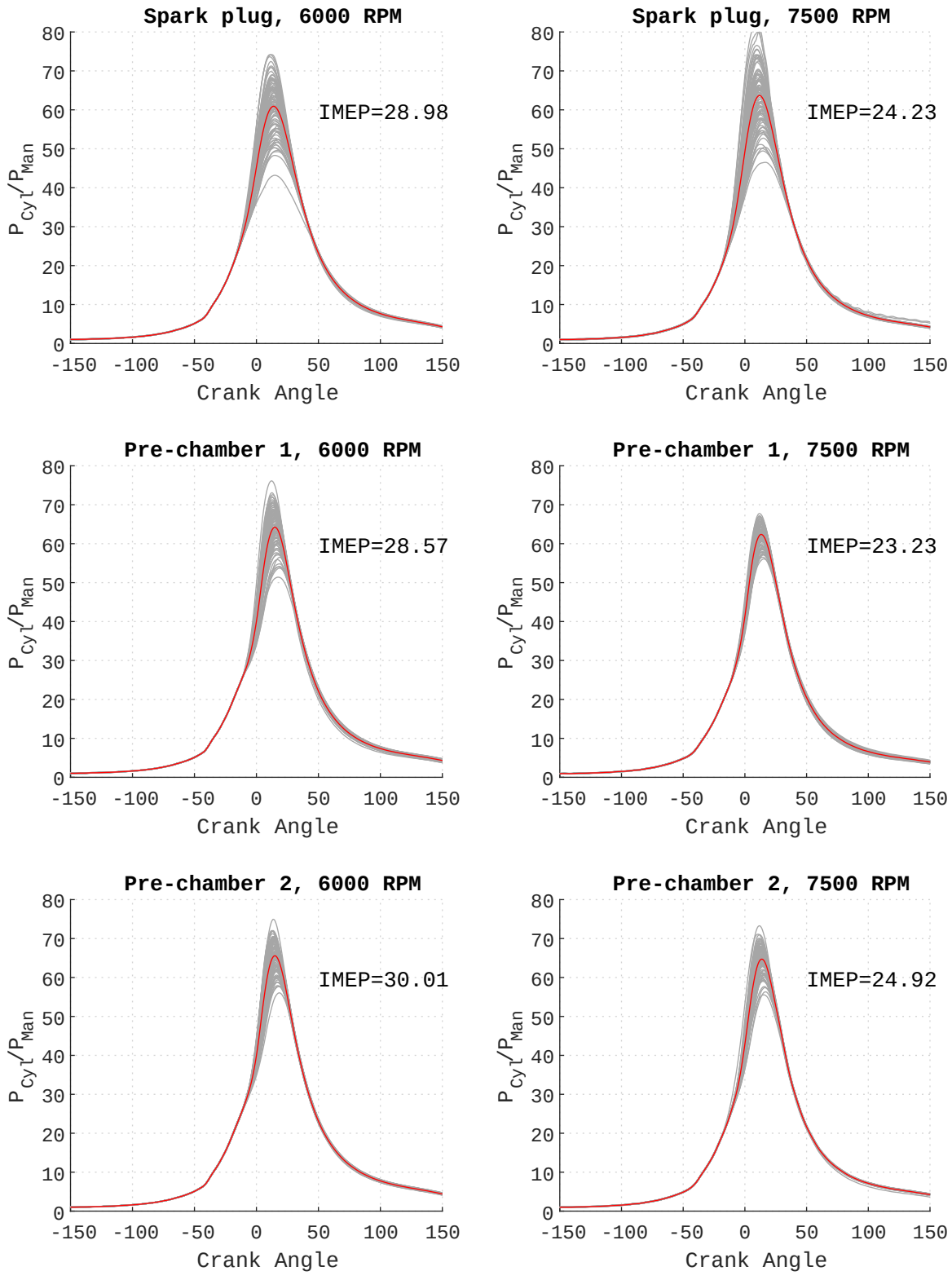

Fig. 20. Measured cylinder pressure comparison for spark plug and two pre-chamber options at $\lambda = 1.2$. 100 cycles data is shown in gray color and average pressure is shown in red color. IMEP is also shown in the respective plots.

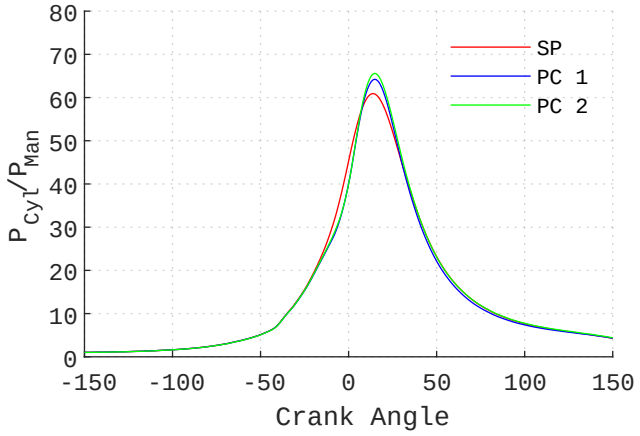

Fig. 21. Measured average cylinder pressure comparison for spark plug and two pre-chamber options at 6000 rpm.

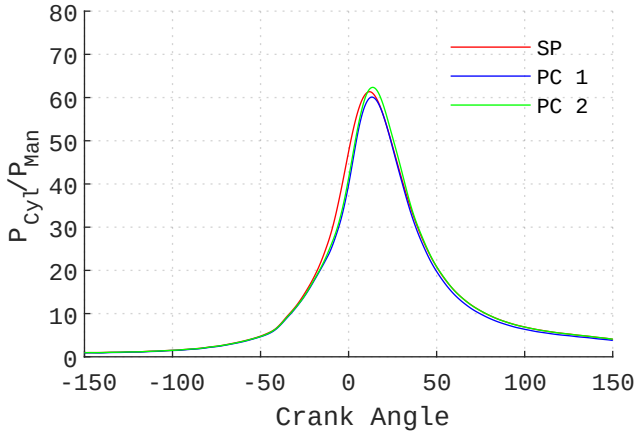

Fig. 22. Measured average cylinder pressure comparison for spark plug and two pre-chamber options at 7500 rpm.

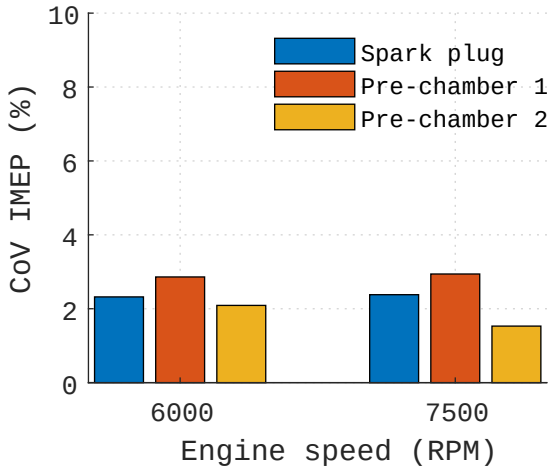

Fig. 23. Coefficient of variation of IMEP

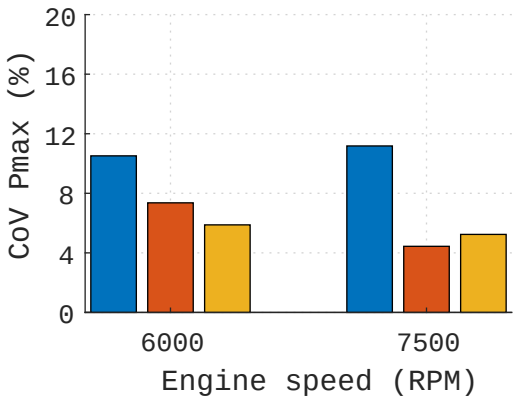

Fig. 24. Coefficient of variation of maximum pressure

compared to the spark plug case, despite having noticeable lower peak pressure variation as shown in Fig. 24. At 6000 rpm, pre-chamber 1 was found to have higher peak pressure compared to spark plug case due to short burn duration, but this higher peak pressure did not convert to gain in IMEP. The reduced IMEP observed with the pre-chamber 1 is a combined effect of higher CoV of IMEP and increased heat transfer loss. To understand influence of heat transfer, calculated mass burnt fraction based on the measured pressure data for all the three cases at 6000 rpm are shown in Fig. 27. With the pre-chamber 1, net heat release was lower for the same fuel energy supplied which indicated higher heat transfer losses. With the pre-chamber 2, heat transfer loss was comparable to the base spark ignition case. It is worth to note that for lean burn combustion, combustion efficiency is close to unity [14] and the difference between fuel energy supplied and energy released (calculated from the pressure data) inside the cylinder is mainly from heat transfer to the walls.

To validate the pre-chamber CFD models, simulated results were compared with the pre-chamber test results. Two cases which achieved correlation and another case which couldn't obtain good correlation are shown in Fig. 28, Fig. 29 and in Fig. 30, respectively. For the Pre-chamber 2, CFD model achieved good correlation to the measured average pressure data. The small discrepancies are attributed to the mismatch of combustion phasing. It is key to note that with a RANS based CFD model, it is difficult to identify ignition timing corresponding to KLSA operating point and to make exact prediction on performance (IMEP). Because, when engine is running at KLSA, a knocking cycle is an extreme variation of the pressure curve, mainly attributed to the lowest ignition delay compared to the other cycles and a RANS model is expected give a pressure curve close to the average pressure curve. So a CFD model is beneficial in predicting the performance of different designs with same ignition timing, and other useful information like pre-chamber fuel enrichment.

For the pre-chamber 1, CFD model over predicts the pressure curve. Higher peak pressure observed with the large volume pre-chamber was not reproduced in the test. This deviation indicates that the CFD model was not able

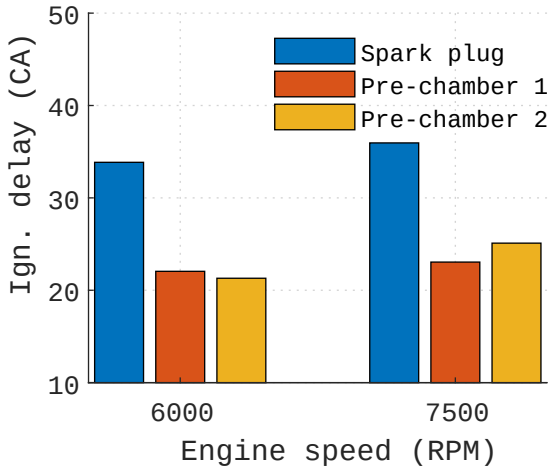

Fig. 25. Ignition delay: Crank angle duration from spark ignition to MBF10%

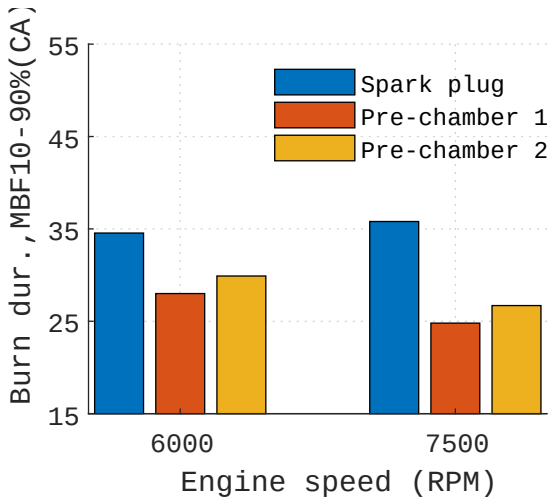

Fig. 26. Crank angle duration from MBF10% to MBF90%

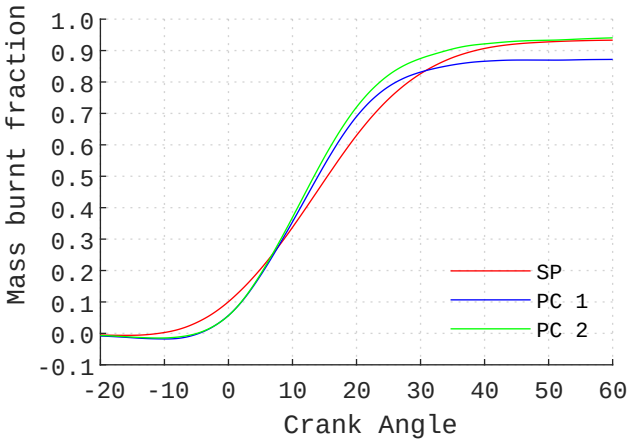

Fig. 27. Measured mass burnt fraction: net heat release normalized by fuel energy supplied, 6000 rpm.

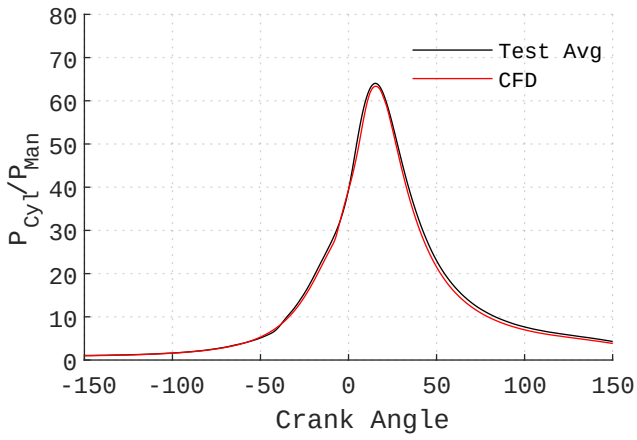

Fig. 28. Correlation of test and CFD results for the pre-chamber design option 2, 6000 rpm

to reproduce the combustion instability associated with lean mixture inside the pre-chamber, observed with the large volume pre-chamber. The spark ignition model used in the CFD model ensured combustion start even with lean mixture and more accurate spark ignition models are required to account for unstable combustion start. So when a pre-chamber is modeled, it is important look at pre-chamber fuel enrichment and thus make an assessment on combustion stability. Though average pressure curve was found to have a higher deviation, there were individual test cycles matching to the predicted pressure curve as shown in the same Fig. 30 and it shows that the predicted pressure curve is realizable if combustion stability can be achieved by having rich mixture inside the pre-chamber.

7 Conclusion

An unsteady RANS based CFD engine model with the detailed chemistry combustion model can aid in the design of combustion devices like pre-chamber. Though, this model has difficulty in accurately predicting the pressure curve with unstable conditions near the spark plug, it can give the indication like mixture state, from which a designer can make a decision on the final design. Pre-chamber enrichment is a key criteria to be looked in a pre-chamber simulation to make a prediction on combustion stability. The CFD based parametric study provides the following guidelines for the pre-chamber design:

Higher pre-chamber volume reduces burn duration, but results in lean burning inside the pre-chamber, leading to the resultant combustion instability.

Number of nozzles and nozzle diameter has to be decided in conjunction with the pre-chamber volume. The criteria is to provide optimum restriction across the nozzles to have sufficient pre-chamber filling and also to build up adequate pressure inside the pre-chamber for high velocity turbulent jet ejection.

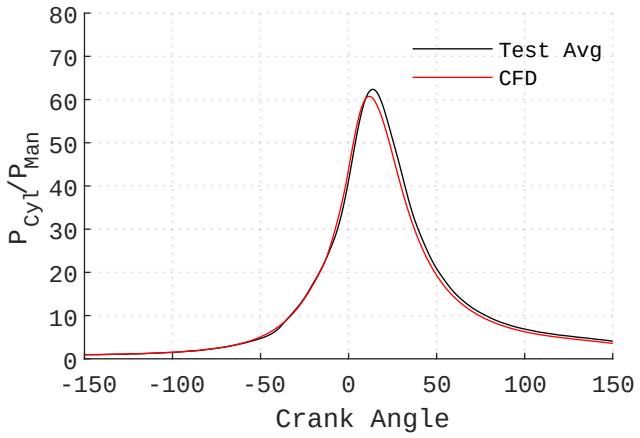

Fig. 29. Correlation of test and CFD results for the pre-chamber design option 2, 7500 rpm

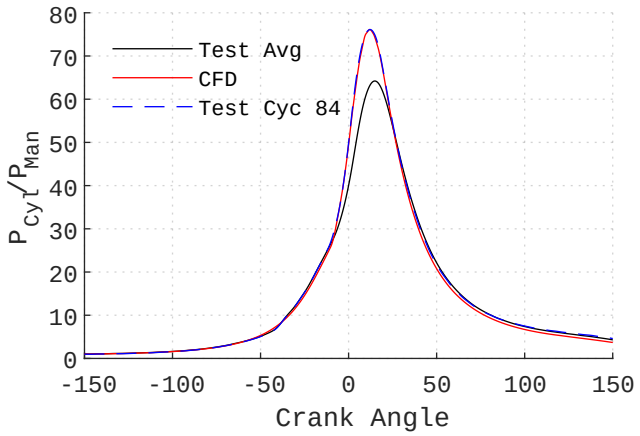

Fig. 30. Correlation of test and CFD results for pre-chamber design option 1, 6000 rpm. A single measured cycle is shown as Test Cyc 84.

Tangential entry nozzle helps in improved mixing inside the pre-chamber and helps in symmetrical jet ejection to the main combustion chamber.

The testing with pre-chamber designs made on above guidelines validated combustion insatiability with a large volume pre-chamber. Higher IMEP and lower CoV in IMEP was achieved with a small volume pre-chamber design, which helped in maintaining rich mixture inside the pre-chamber. Testing results also show that with a large volume pre-chamber, heat transfer loss was increased, resulting in reduced work output.

The work presented in this paper is planned be continued with investigation of combustion chamber design with the aim being to ensure fuel enrichment inside the pre-chamber, especially with increased dilution and a review of the current port induced tumble generation and turbulent combustion, which was originally optimised for spark plug initiated combustion. As the engine achieved MBT operating points with the pre-chamber ignition system, as shown in the work presented in this paper, further tests need to be conducted with a higher compression ratio to investigate potential gains towards a higher thermal efficiency. A cylinder pressure based knock detection method is also to be identified for final implementation of the pre-chamber ignition system as the current accelerometer based knock detection strategy was found to output false positives for knocking cycles, as observed in the current study in this paper.

Acknowledgements

Advanced Engine Research Ltd (UK) is acknowledged for their sponsorship and providing design and manufacturing support for this research project. Convergent Science Inc. is acknowledged for providing CONVERGE CFD software academic license. AVL is also acknowledged for providing AVL CONCERTO 5 academic license.

References

[1] Whiting, C., 2018. FIA Formula one world championship regulations.

[2] International Energy Agency, 2012. Energy Technology Perspectives 2012: Pathways to a Clean Energy System. Tech. rep., International Energy Agency.

[3] Ulrich, S., Steffen, E., and Ansgar, C., 2017. "Roadmap to a de-fossilized powertrain". In Internationales Stuttgarter Symposium: Automobil und Motorentechnik 2017, Springer.

[4] Toulson, E., Schock, H. J., and Attard, W. P., 2010. "A review of prechamber initiated jet ignition combustion systems". *SAE Technical Paper,* **2010-01-22**.

[5] Toulson, E., and Thelen, B. C., 2016. "A computational study on the effect of the orifice size on the performance of a turbulent jet ignition system". *Proceedings of the Institution of Mechanical Engineers, Part D: Journal of Automobile Engineering*, aug.

[6] Thelen, B. C., and Toulson, E., 2016. "A Computational Study of the Effects of Spark Location on the Performance of a Turbulent Jet Ignition System". *SAE Technical Paper,* **2016-01-06**.

[7] Gussak, L. A., Turkish, M. C., and Siegla, D. C., 1975. "High Chemical Activity of Incomplete Combustion Products and a Method of Prechamber Torch Ignition for Avalanche Activation of Combustion in Internal Combustion Engines". *SAE Technical Paper,* **750890**.

[8] Kettner, M., Rothe, M., Velji, A., Spicher, U., Kuhnert, D., and Latsch, R., 2005. "A new flame jet concept to improve the inflammation of lean burn mixtures in SI engines". *SAE Technical Paper,* **2005-01-36**.

[9] Attard, W. P., and Blaxill, H., 2011. "A Single Fuel Pre-Chamber Jet Ignition Powertrain Achieving High Load, High Efficiency and Near Zero NOx Emissions". *SAE International Journal of Engines,* **2011-01-20**.

[10] Attard, W. P., Blaxill, H., Anderson, E. K., and Litke, P., 2012. "Knock Limit Extension with a Gasoline Fu-

eled Pre-Chamber Jet Igniter in a Modern Vehicle Powertrain". *SAE International Journal of Engines,* **2012-01-11**.

[11] Attard, W. P., and Blaxill, H., 2012. "A Lean Burn Gasoline Fueled Pre-Chamber Jet Ignition Combustion System Achieving High Efficiency and Low NOx at Part Load". *SAE International Journal of Engines,* **2012-01-11**.

[12] Attard, W. P., and Blaxill, H., 2012. "A Gasoline Fueled Pre-Chamber Jet Ignition Combustion System at Unthrottled Conditions". *SAE International Journal of Engines,* **2012-01-03**.

[13] Attard, W. P., Fraser, N., Parsons, P., and Toulson, E., 2010. "A Turbulent Jet Ignition Pre-Chamber Combustion System for Large Fuel Economy Improvements in a Modern Vehicle Powertrain". *SAE Technical Paper,* **2010-01-14**.

[14] Heywood, J. B., 2006. *Internal combustion engine Fundamentals*, Vol. 21.

[15] Geiger, J., Pischinger, S., and Böwing, R., 1999. "Ignition Systems for Highly Diluted Mixtures in SI-Engines". *SAE Technical Paper,* **1999-01-07**.

[16] Stone, R., 2012. *Introduction to Internal Combustion Engines*, 4 ed. Palgrave Macmillan.

[17] Ozdor, N., Dulger, M., and Sher, E., 1994. "Cyclic Variability in Spark Ignition Engines A Literature Survey". *SAE Technical Paper,* **940987**.

[18] Truffin, K., Angelberger, C., Richard, S., and Pera, C., 2015. "Using large-eddy simulation and multivariate analysis to understand the sources of combustion cyclic variability in a spark-ignition engine". *Combustion and Flame,* **162**, pp. 4371–4390.

[19] Young, M. B., 1981. "Cyclic Dispersion in the Homogeneous-Charge Spark-Ignition Engine—A Literature Survey". *SAE Technical Paper,* **810020**.

[20] Chinnathambi, P., Bunce, M., and Cruff, L., 2015. "RANS Based Multidimensional Modeling of an Ultra-Lean Burn Pre-Chamber Combustion System with Auxiliary Liquid Gasoline Injection". *SAE 2015 World Congress and Exhibition,* **2015-01-03**.

[21] Adomeit, P., Lang, O., Pischinger, S., Aymanns, R., Graf, M., and Stapf, G., 2007. "Analysis of Cyclic Fluctuations of Charge Motion and Mixture Formation in a DISI Engine in Stratified Operation". *SAE Technical Paper,* **2007-01-14**.

[22] Goryntsev, D., Sadiki, A., Klein, M., and Janicka, J., 2009. "Large eddy simulation based analysis of the effects of cycle-to-cycle variations on air-fuel mixing in realistic DISI IC-engines". *Proceedings of the Combustion Institute,* **32**.

[23] Richards, K. J., Senecal, P. K., and Pomraning, E., 2018. *CONVERGE 2.4 Manual*. Convergent Science, Madison, WI (2018).

[24] Senecal, P. K., Pomraning, E., and Richards, K. J., 2003. "Multi-dimensional modeling of direct-injection diesel spray liquid length and flame lift-off length using CFD and parallel detailed chemistry". *SAE Technical Paper 2003-01-1043*.

[25] Robert, J., 1991. "Chemkin-II: A Fortran chemical kinetics package for the analysis of gas-phase chemical kinetics". *Sandia National Laboratories Report*.

[26] Liu, Y. D., Jia, M., Xie, M. Z., and Pang, B., 2013. "Development of a new skeletal chemical kinetic model of toluene reference fuel with application to gasoline surrogate fuels for computational fluid dynamics engine simulation". *Energy and Fuels*.

[27] Marinov, N. M., 2002. "A detailed chemical kinetic model for high temperature ethanol oxidation". *International Journal of Chemical Kinetics*.

[28] Budak, O., Hoppe, F., Heuser, B., Pischinger, S., Burke, U., and Heufer, A., 2018. "Hot surface pre-ignition in direct-injection spark-ignition engines: Investigations with Tailor-Made Fuels from Biomass". *Special Issue Article International J of Engine Research,* **19**(1), pp. 45–54.

[29] Pomraning, E., Richards, K., and Senecal, P. K., 2014. "Modeling Turbulent Combustion Using a RANS Model, Detailed Chemistry, and Adaptive Mesh Refinement". *SAE Technical Paper Series,* **1**.

[30] Granet, V., Vermorel, O., Lacour, C., Enaux, B., Dugué, V., and Poinsot, T., 2012. "Large-Eddy Simulation and experimental study of cycle-to-cycle variations of stable and unstable operating points in a spark ignition engine". *Combustion and Flame,* **159**, pp. 1562–1575.

[31] Richards, K., Pomraning, E., and Probst, D., 2014. "The Observation of Cyclic Variation in Engine Simulations When Using RANS Turbulence Modeling". *Proceedings of the ASME 2014 Internal Combustion Engine Division Fall Technical Conference*, pp. 1–19.

[32] Jupudi, R. S., Finney, C. E., Primus, R., Wijeyakulasuriya, S., Klingbeil, A. E., Tamma, B., and Stoyanov, M. K., 2016. "Application of High Performance Computing for Simulating Cycle-to-Cycle Variation in Dual-Fuel Combustion Engines". In SAE Technical Papers.

[33] Scarcelli, R., Richards, K., Pomraning, E., Senecal, P. K., Wallner, T., and Sevik, J., 2016. "Cycle-to-Cycle Variations in Multi-Cycle Engine RANS Simulations". *SAE Technical Papers*.